Reaction Chemistry & Engineering

ROYAL SOCIETY OF CHEMISTRY

PAPER

View Article Online
View Journal | View Issue

Check for updates

Cite this: *React. Chem. Eng.*, 2021, **6**, 2114

Tailored monolith supports for improved ultra-low temperature water-gas shift reaction†

Raquel Portela, ‡*[a] Patrick Wolf,‡[b] Jakob M. Marinkovic, [c] Ana Serrano-Lotina,[a] Anders Riisager [c] and Marco Haumann *[b]

Received 7th June 2021,
Accepted 2nd August 2021

DOI: 10.1039/d1re00226k

rsc.li/reaction-engineering

Supported ionic liquid-phase (SILP) particulate catalysts consisting of Ru-complexes dissolved in an ionic liquid that is dispersed on a γ-alumina porous substrate facilitate the water-gas shift (WGS) reaction at ultra-low temperatures. In this work, a screening of different ceramic support materials was performed to design a suitable monolithic support to disperse the SILP system with the objective of scaling up the WGS process efficiently. γ-Alumina-rich channeled monoliths were developed with the use of natural clays as binders (10 wt% bentonite and 20 wt% sepiolite) with the following properties: i) high volume of mesopores to maximize the catalyst loading and successfully immobilize the ionic liquid-catalyst system *via* capillary forces, ii) mechanical resistance to withstand the impregnation process and the reaction operating conditions, and iii) surface chemistry compatible with a highly active and selective phase for WGS. The developed monolithic-SILP catalyst demonstrated high stability and long-term WGS performance at 130 °C with an average steady-state CO conversion of around 30% after 190 h time-on-stream (TOS) and a conversion of 23% after 320 h TOS. Interestingly, the catalyst activity proved essentially unaffected by variation in the water partial pressure during operation due to accumulation of water in the monolith, thus making the system highly durable.

1 Introduction

Hydrogen is an important and indispensable reactant in established processes such as hydrocracking, ammonia or methanol production.[1,2] The use of renewable energy can help to produce hydrogen in a more sustainable and benign way. However, today the vast majority of H_2 (over 95%) is still obtained from fossil fuels by reforming processes. In these processes carbon monoxide (CO) is formed inevitably, which constitutes a severe catalyst poison and hence has to be removed for applications such as proton-exchange membrane fuel cells or iron-catalyzed ammonia synthesis.[3,4] Therefore, the water-gas shift (WGS) reaction of CO and H_2O to form CO_2 and H_2 (see Scheme 1) is an essential intermediate step of current industrial H_2 production.

State-of-the-art WGS industrial processes are heterogeneously catalyzed and typically carried out in two consecutive steps.[5] The first high-temperature WGS step brings down CO levels to approx. 3 vol%, using Fe_2O_3/Cr_2O_3 catalysts around 450 °C. At lower temperatures of 200 °C $CuO/ZnO/Al_2O_3$ catalysts bring down the CO level as low as 0.3 vol% (*i.e.* 3000 ppm). Additional energy- and cost-intensive purification steps are indispensable to further reduce CO concentration for applications that require high-purity hydrogen. Heterogeneous catalysts cannot reduce the rather high CO level of approx. 3000 ppm further, since such catalysts are strongly limited kinetically at temperatures below 200 °C. In contrast, homogeneous transition metal complexes have been reported to be active even at temperatures well below 200 °C.[6] At such ultra-low temperatures the thermodynamics would allow further reduction of CO levels to acceptable values below 10 ppm. However, these homogeneous complexes require rather harsh reaction conditions in terms of pressure and use of strong bases, making such processes less viable for continuous WGS. In recent years, the concept of supported ionic liquid-phase (SILP) catalysis has proven to be a promising way to overcome such limitations.[7] In SILP materials, the homogeneous Ru-complexes are dissolved in an ionic liquid (IL) that is dispersed on a γ-alumina porous substrate.[8,9] The resulting material appears solid on a macroscopic level, while on the microscopic level the catalyst operates inside the thin ionic liquid film. The high gas–liquid interface minimizes transport limitations typically associated with ionic liquids. SILP

[a] *CSIC – Consejo Superior de Investigaciones Científicas, Madrid, Spain. E-mail: raquel.portela@csic.es*
[b] *Lehrstuhl für Chemische Reaktionstechnik, Friedrich-Alexander-Universität Erlangen-Nürnberg, Egerlandstraße 3, D-91058 Erlangen, Germany. E-mail: marco.haumann@fau.de*
[c] *Centre for Catalysis and Sustainable Chemistry, Department of Chemistry, Technical University of Denmark, Kemitorvet, Building 207, 2800 Kgs. Lyngby, Denmark*

† Electronic supplementary information (ESI) available. See DOI: 10.1039/d1re00226k

‡ Authors contributed equally.

$$H_2O + CO \rightleftharpoons H_2 + CO_2 \qquad \Delta H_R = -41.2\,kJ\,mol^{-1}$$

Scheme 1 Reaction equation of the water-gas shift (WGS) reaction.

catalysts for WGS have so far mainly been applied on grains of micro- to millimeter scale, making the heat management and upscaling of such packed-bed reactors challenging.[10,11] Previously, some of us reported a first upscaling approach consisting of Ru–carbonyl complexes in $[C_4C_1C_1Im]Cl$ (1-butyl-2,3-dimethylimidazolium chloride) immobilized on mesoporous alumina particles of 200–500 μm filling the channels of a 200-mm-long silica-washcoated silicon carbide (SiO_2/SiC) macroporous monolith (see "Previous work" in Fig. 1).[12]

This arrangement of SILP particles resembled a multi-tubular reactor configuration, in which the high heat conductivity of the SiC allowed efficient heat removal and close to isothermal operation. For heterogeneous WGS systems such improved heat distribution inside monolithic reactors has been reported as well.[13,14] In the ultra-low temperature monolithic SILP arrangement, the outer surface of the monolith was coated with a membrane, allowing preferential CO_2 removal *via* a facilitated transport mechanism. While this first proof of a two-in-one SILP membrane reactor was successful, the utilization of the SiC monolith was rather poor, since the active species was located in the channels rather than inside the porous monolith structure itself. The incorporation of the thin ionic liquid film into the monolithic structure as proposed in this work is highly beneficial,[15] as intrinsic kinetics, fluid dynamics, and transport phenomena can be optimized independently in such structured reactors,[16] and modeling, scale-up, and process control are simplified. Very recently, some of us have successfully applied this approach for but-1-ene hydroformylation,[17] showing stable and efficient operation over 40 h time-on-stream (TOS) using the same SiO_2-washcoated SiC monoliths[18] as support to immobilize Rh–diphosphite complexes.[19] A high pressure-drop was avoided by the macroporosity as well as the channeled design of the structure, and the SiC provided heat conductivity, mechanical strength, and chemical inertness.[20]

The application of the ultra-low temperature WGS SILP catalyst system directly onto a porous monolithic support is challenging due to the reaction conditions. At such low temperatures, the water vapor can condense inside the porous network. If the capillary forces retaining the ionic liquid are too weak due to large macro-pores, unwanted leaching of the catalyst system can occur easily.[21] If this is the case, new tailor-made porous monoliths have to be developed. The objective of this work is to apply this novel SILP approach based on the immobilization of the catalyst-containing ionic liquid on a structured support to the WGS reaction.

2 Experimental

2.1 Materials

WGS SILP catalysts were prepared and tested as i) particles, for supporting material screening against benchmark

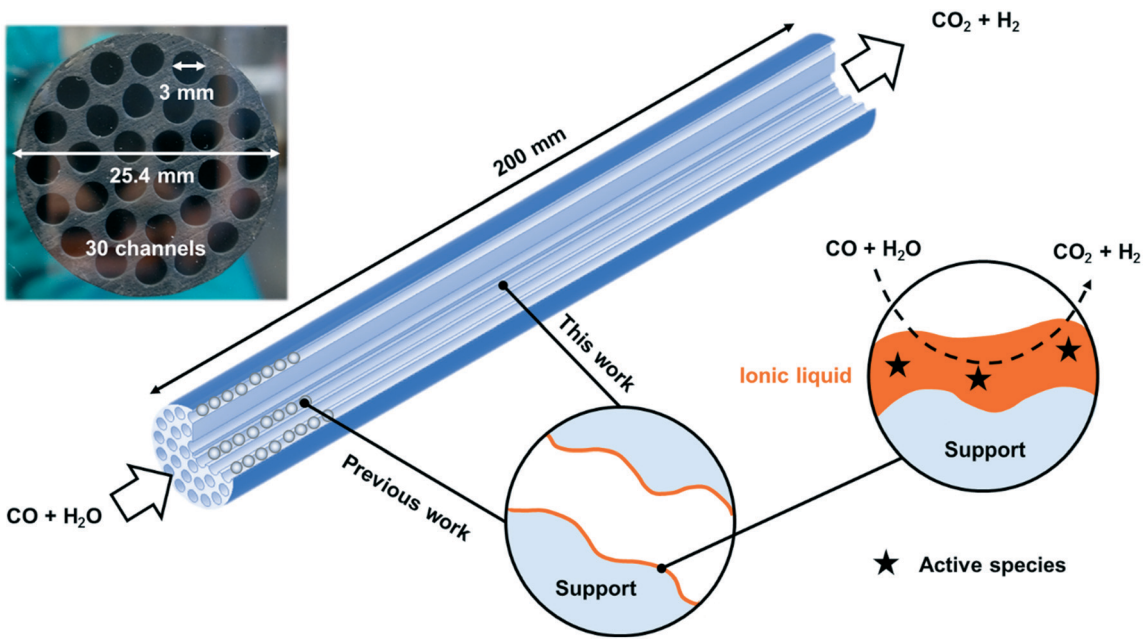

Fig. 1 Schematic representation of the concept of supported ionic liquid-phase (SILP) catalysis applied to monolithic support structures. Monolith dimensions are shown in the picture. Previous work investigated the placement of SILP particles inside the channels of a SiO_2-washcoated SiC monolith.[12] This work reports on the impregnation of an entire monolith structure.

γ-alumina, and ii) channeled monoliths, for the monolithic-SILP concept validation for this reaction. γ-Al_2O_3 (Sasol Germany GmbH) were fractioned to 200–500 μm to be used as reference support to prepare the benchmark WGS SILP catalytic system.[22,23] For the screening of new extruded support materials, extrudates were prepared, crushed and sieved to the same particle fraction of 200–500 μm as the benchmark alumina particles. The ionic liquid 1-butyl-2,3-dimethylimidazolium chloride ([$C_4C_1C_1$Im]Cl, >97%) was purchased from Merck KgaA, dichloromethane (DCM, ≥99.9%) from Sigma-Aldrich, and the ruthenium precursors $RuCl_3$ (99.9%) and the dimer $[Ru(CO)_3Cl_2]_2$ (>98%) from Best Chemicals and Alfa Aesar, respectively. All chemicals were used as received and the catalysts prepared under an inert atmosphere (Ar 99.999 vol%) using standard Schlenk techniques.

2.2 Preparation of particulate SILP catalysts

A Ru catalyst-containing ionic liquid stock solution for impregnation of the particles was prepared as follows: A desired amount of [$C_4C_1C_1$Im]Cl was dissolved in 15 mL DCM and stirred for 15 min, followed by addition of a solution of a desired amount of $[Ru(CO)_3Cl_2]_2$ dissolved in 10 mL DCM. Next, the respective support material was added to the solution and stirring stopped after 2–5 min to avoid mechanical stress on the support. The DCM was slowly removed under reduced pressure at room-temperature, and the resulting free-flowing and dry SILP catalyst particles were stored under an argon atmosphere prior to use. The theoretical Ru loading of the SILP catalyst was w_{Ru} = 0.02 g_{Ru} $g_{support}^{-1}$, and the pore filling degree of the support, described as the ionic liquid volume related to the total pore volume of the support material (V_{IL} $V_{support}^{-1}$), was α = 0.34, the optimal value for such catalysts.[24]

2.3 Preparation of monolithic SILP catalysts

Two different types of monolithic-SILP catalysts were developed in this work: i) the SiO_2/SiC monolith used in previous SILP approaches was impregnated with the thin WGS catalyst-containing ionic liquid film, and ii) new extrudable support materials were screened for improved monolithic-SILP design. The most promising new material was finally shaped into the same geometry as the SiO_2/SiC monolith for impregnation. The dimensions of the monoliths were 200 mm length, 25.4 mm diameter, and 30 channels of *ca.* 3 mm inner diameter.

2.3.1 SiO_2/SiC monolith. The commercial SiC monoliths (see insert in Fig. 1, LiqTech International A/S) were manufactured by sintering α-SiC powder (particle diameter 17.3 μm), resulting in fully recrystallized monoliths. Afterwards, an outer support layer consisting of sub-micrometer sized α-SiC particles was applied to create a homogeneous surface, and finally the structure was washcoated with 7 nm SiO_2 particles to provide an improved interface with the catalyst.[18]

2.3.2 New mesoporous supports. Pure γ-alumina mesoporous monoliths with the geometry required for this work were obtained by mechanical extrusion and subsequent calcination at 550 °C using boehmite as alumina precursor, water as peptizing agent, and additives, as described elsewhere.[25] Additionally, alumina-rich extrudates were prepared with different proportions of bentonite, a 2 : 1 phyllosilicate with ideal formula $(Na,Ca)_{0.33}(Al,Mg)_2(Si_4O_{10})$; fibrous sepiolite, with general formula $Mg_4Si_6O_{15}(OH)_2{\cdot}6H_2O$; and/or kaolinite, 1 : 1 phyllosilicate with ideal formula $Al_2Si_2O_5(OH)_4$, for new composition screening, as these provide very good mechanical stability, mesoporosity, and plasticity, respectively. The main properties of the binders are collected in Table S1.†

As reference, the clays were first extruded as single-component pellets and monoliths and calcined at 550 °C. Sepiolite was selected among them to test the effect of the calcination temperature, textural properties and naturally present impurities. For that purpose, sepiolite pellets were calcined at different temperatures and extruded with higher (>85%) and lower (60%) purity, as well as with and without extra macroporosity created by hard templating. The selected pore generation agent (PGA), activated carbon, was added to the extrusion dough and burnt during the calcination step. Different combinations of these binders with the alumina precursor and water were extruded manually as cylindrical pellets. In addition, alumina-free, carbon-containing extrudates were also prepared mixing activated carbon and sepiolite binder to be tested as alternative supports; kaolinite, used to improve the extrusion properties, was either added or left out. All the materials were heat treated in inert atmosphere to avoid the combustion of the activated carbon.

The best support composition was shaped as full monolith. First, the mixture of silicates and the boehmite were properly blended in a mixer and then water was added until adequate plasticity was obtained. The plastic formulation was shaped in a mechanical extruder into the 30-channel cylindrical monolith. The extrusion die was designed considering the material shrinkage after drying and calcination (see Fig. S6†) to obtain final diameters of *ca.* 25.4 mm for the external wall and 3 mm for the channels. The monoliths were finally cut to a length of 200 mm.

Regarding the nomenclature of the as prepared materials, the extrudate sample names contain a number indicating the wt% of the component in the final calcined support followed by the component identifier: Al stands for γ-alumina formed by calcination of commercial high purity boehmite (Pural® SB1, Sasol), S and S9 refer to sepiolite Pansil 100 (60% purity) and Pangel S9 (purity >85%), respectively (both from Tolsa S. A.). B indicates bentonite (Pangel M280, Tolsa S.A.), K refers to kaolinite (Hymod Excelsior, ECC/Imerys), C to unburned activated carbon (samples heat treated in inert flow), and PGA to activated carbon removed by calcination at 550 °C to generate extra macroporosity. The standard temperature for calcination was 550 °C for 4 h. If a number is added at the end of the sample name, it represents a calcination temperature different than 550 °C.

2.3.3 Impregnation of the monoliths. For the wet-impregnation of the ceramic monoliths a stock solution of the catalyst system was prepared by dissolving 19.55 g of $[C_4C_1C_1Im]Cl$ in 100 ml of DCM followed by 15 min stirring. Thereafter, 5.98 g of $[Ru(CO)_3Cl_2]_2$ or 4.84 g of $RuCl_3$, dissolved in 10 ml of DCM, were added and the solution was stirred for 5 min before the final addition of 52 ml of DCM. Beside a literature known induction period, the performance of $RuCl_3$ precursor is the same compared to $[Ru(CO)_3Cl_2]_2$ with both transforming into $[Ru(CO)_3Cl_3]^-$ as the main active species during operation.[9,26] The catalyst solution was stirred for 2 h prior to monolith impregnation resulting in a homogeneous stock solution containing an IL-to-Ru molar ratio of 4.4 and an α_{IL} value of approx. 0.1.

The monoliths were submerged in the homogeneous catalyst stock solution for 5–6 min before removal of the liquid by draining the stock solution out of the channels. The monoliths were then dried at room temperature in two steps, first under an argon flow for 24 h and subsequently under vacuum for 24 h. The final Ru content in the monoliths was determined indirectly by the weight gain resulting from the impregnation process, assuming a homogeneous catalyst stock solution and a total removal of the solvent.

2.4 Characterization

Textural characterization of the composites was obtained on degassed samples from N_2 adsorption/desorption isotherms measured at −196 °C with an ASAP 2420 apparatus (Micromeritics) and from mercury intrusion porosimetry (MIP) performed using an AutoPore IV 9510 mercury intrusion/extrusion porosimeter (Micromeritics). Specific surface area data was calculated by application of the BET equation to the N_2 adsorption isotherm, and the external surface area from MIP measurement. Pore volume and pore size distribution curves combine data from MIP (in the meso- and macropore range) and N_2 isotherms (micro- and mesopore range). Pore size was calculated using the Washburn equation for cylindrical pores.

The crystalline structure of the support was evaluated by X-ray diffraction (XRD) with a PANalytical X'Pert Pro diffractometer using Ni-filtered Cu K_α radiation with λ = 1.5406 nm.

Thermogravimetric analysis (TGA) were performed with *ca.* 25 mg samples under air flow of 50 mL_N min^{-1} with a heating rate of 10 °C min^{-1} in the range 25–900 °C using a STA 6000 equipment (Perkin Elmer).

The crushing strength of samples was measured with a Chatillon dynamometer. The measurements were repeated at least ten times on various samples to secure statistically significant values. The structural resistance of the plates to water and to DCM was tested immersing the samples in each of the solvents for 15 min.

Chemical analysis was obtained by inductively coupled plasma atomic emission spectroscopy (ICP-AES) using a Ciros CCD (Spectro Analytical Instruments GmbH). The solid samples were treated with a mixture of concentrated HCl : HNO_3 : HF using microwave heating up to 220 °C for 40 min to dissolve all material for the analysis (the mixture was prepared based on volumetric ratios; CAUTION: HF is extremely harmful, relevant safety precautions must be taken). The instrument was calibrated with standard solutions of Ru prior to the measurements.

Qualitative analysis for chloride ions in the condensate was performed using silver nitrate solution and nitric acid.

2.5 Catalytic experiments using SILP particles

The catalytic experiments for the SILP particles were carried out in a packed-bed reactor setup (1.4571 stainless steel) with an inner diameter of 10 mm and a total volume of 26 mL. The reactor and its periphery are depicted in Fig. S1.† The catalyst samples were placed on a 0.5 μm frit to avoid particles from entering the downstream section of the test rig. The gases CO (99.97%, Linde AG) and N_2 (99.999%, Linde AG) were dosed *via* mass-flow controllers (MFC). Water was dosed with a liquid-flow controller and mixed with N_2 utilizing a controlled evaporator mixer (CEM) unit from Bronkhorst. The gas mixture consisting of N_2, CO and water passed through either a bypass-line or the reactor, and then through a condenser unit (T = 1.5 °C). Finally, the dry gas composition was analyzed on-line using an Emerson X-Stream gas analyzer. After a ramp-up phase applying a low N_2 flow (F_{N_2} = 50 mL_N min^{-1}) up to 120 °C, the reaction mixture was directed through the bypass-line to gain a reference point for the calculation of the catalytic activity. Subsequently, the gas stream was sent through the fixed-bed reactor for temperature-programmed activity measurements between 120–140 °C in 5 °C steps and 5 h dwell time, so that the total time-on-stream was 45 h. A by-pass reference measurement was made in-between each temperature. Exemplary results of such a typical catalytic experiment can be found in Fig. S7.† All the screenings were performed using 2.0 g of supported catalyst.

2.6 Catalytic experiments using monolithic-SILP

The experiments with the extruded and impregnated monoliths were carried out in an in-house designed reactor consisting of a reactor pipe (1.4571 stainless steel) with an outer diameter of 50 mm with fixed flanges on both sides. The reactor and its periphery are depicted in Fig. S2.† The monolith was fixed within the reactor using supporting rings. To compensate slight changes in the length of the monoliths, a distance ring was used in the lower flange. The heat was evenly distributed using aluminum half-shells placed around the mounted reactor. Further information about the setup can be found elsewhere.[12]

Reaction gas flows were controlled by MFCs from Bronkhorst, while water was fed into the system through an evaporation section using an HPLC pump from Techlab (OEM mini pump, micro pump head, F_{H_2O} = 10 μL min^{-1} – 2 mL min^{-1}) and nitrogen as carrier gas. The gas mixture, consisting

of water vapor, nitrogen and CO could either be fed through the bypass line or the reactor, after which a condenser unit was installed (glass coil cooler). The condenser unit was cooled to 1 °C using a cryostat from Huber (Minichiller 300); condensed water was led to a flask via a PTFE tube. The dry gas was directed to the online IR analyzer (Emerson X-Stream). The temperature in the various sections was controlled and regulated by thermocouples and controllers from Eurotherm. Also, thermocouples were attached to various potential cold spots in order to monitor the temperature and prevent unwanted condensation of water. The periphery was heated to a temperature of 140–160 °C to ensure no condensation. A more detailed description of the setup and the respective parts can be found in literature[12] and the ESI.†

2.7 Calculation of the catalytic activity

SILP catalyst activity was calculated based on the turnover frequency (TOF) shown in eqn (1), where $\dot{n}_{\text{product}}$ and n_{catalyst} are the molar flow of CO_2 and the mol of Ru in the sample, respectively.

$$\text{TOF} = \frac{\dot{n}_{\text{product}}}{n_{\text{catalyst}}} \quad (1)$$

The TOF was modified according to eqn (2) because the molar flow of product could not be determined with high accuracy due to the change of the total flow caused by the condensation of water before the online IR-analyzer.

$$\text{TOF} = \frac{\dot{n}_{\text{substrate}} \cdot X_{\text{substrate}}}{n_{\text{catalyst}}} \quad (2)$$

The molar flow of the substrate (CO) was easily calculated from the volume flow of the calibrated MFC and its conversion (X) from the concentration in the inlet and the outlet. The maximum overall error for the catalyst activity amounted to ±5% and error bars have been omitted in the figures for sake of clarity. A more detailed description of the evaluation procedure can be found elsewhere.[22,23]

3 Results and discussion

3.1 Evaluation of commercial SiC monolithic support

SiC monoliths offer several advantages as support for SILP catalysis, in particular chemical inertness, *e.g.* against corrosive intermediates, and high thermal conductivity (200 W mK^{-1})[27] compared to that of benchmark alumina supporting material (14–30 W mK^{-1}),[28] which improves the heat management in the reactor. Hence, the previously reported silica-washcoated commercial SiC monoliths were functionalized for the exothermic WGS reaction *via* a dip coating procedure.[12,17] The experimental activity results for the SILP supported on the SiO_2/SiC monolith are shown in Fig. 2.

During the first 100 h time-on-stream, the catalyst showed a constant positive increase in activity (see Fig. 2 top). This activation phase is well known for such Ru-SILP WGS catalysts and stems from the slow formation of active species accompanied by the formation of a stable IL/water film over the entire support surface.[9] After 100 h it seemed as if the system had stabilized and a step-wise temperature variation between 120 and 160 °C was performed. Once the temperature equilibrated at each stage, the CO conversion quickly became stable as well, with a maximum of 70% at 160 °C. Interestingly, after the temperature again was reduced to 120 °C, the same

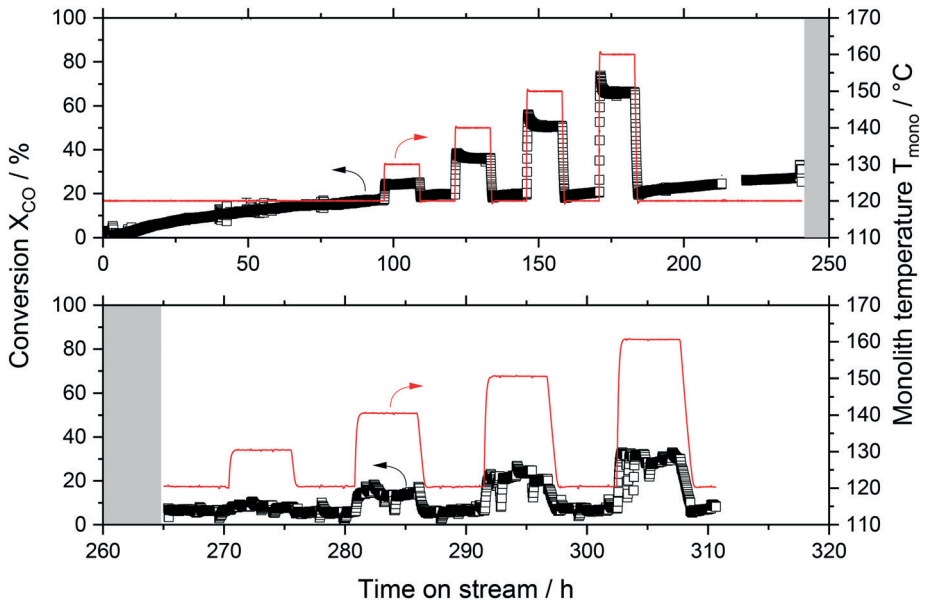

Fig. 2 Conversion (black squares, left axis) and temperature inside the SiC monolith (red line, right axis) over the first 250 h (top) and additional 60 h (bottom) time-on-stream. Nitrogen purge period (200 mL_N min^{-1}) is indicated by the grey areas. T = 120–160 °C, p(abs) = 1 bar, precursor = $RuCl_3$, $m_{\text{precursor}}$ = 0.76 g, IL = $[C_4C_1C_1Im]Cl$, V_{IL} = 2.3 mL, $p_{H2O}:p_{CO}$ = 2 : 1, F_{total} = 174 mL_N min^{-1}.

conversion of *ca.* 18% was obtained as before the temperature variation. However, this conversion continued to increase over the next 70 h to approx. 30%, indicating that the system had not been in stable operation yet. The system was then purged with nitrogen (200 mL_N min^{-1}) for 25 h while the reactor temperature was kept constant at 120 °C. When the feed was switched again to the previous reaction conditions, the activity of the monolith had declined drastically to conversion values as low as 7% at 120 °C and 25% at 160 °C, a reduction by more than 75%. Furthermore, the operation of the system became unstable with high fluctuations, and no steady-state was reached during the next 45 h time-on-stream (see Fig. 2 bottom). After 310 h the reaction was stopped, cooled down and the reactor module dismantled. Severe pitting and corrosion were observed in various locations of the reactor, especially in the bottom part (see Fig. S3†). The change in the color of the monolith during the experiment from reddish-brown to light grey (see Fig. S3†) evidenced leaching of the active phase from the monolith. Given the highly hygroscopic nature of $[C_4C_1C_1Im]Cl$, significant amounts of water dissolved in the IL, leading to swelling. Strong capillary forces inside small mesopores might prevent the removal of this aqueous IL film from the pores, but the large macropores of the SiC monolith[18] could not fulfill this task of proper IL film fixation. As a result, the chloride-containing IL–metal-complex solution leached from the monolith and corroded the reactor material and its downstream section (*e.g.* by release of HCl).[29] These findings are clear evidence that a monolithic support must contain smaller pores to prevent leaching, while at the same time its surface chemistry must facilitate the WGS catalysis, hence, it should be basic. To find materials with these specifications, a support screening was carried out.

3.2 Composition screening of novel monolithic supports

A screening of differently shaped supports with high pore volume and small mesopores was performed to maximize the catalyst loading and to avoid leaching by successful immobilization of the active phase *via* capillary forces. Additionally, the composition was optimized to obtain mechanical resistance and a surface chemistry compatible with a highly active and selective IL-catalyst system for WGS. Several support materials were investigated, ranging from carbon-based to γ-Al_2O_3-based ones, using bentonite, sepiolite and kaolinite natural clays as binders. For this purpose, extrudability, impregnation and catalytic activity tests were performed, the details of the composition selection can be found in the ESI† (see section "Novel monolithic supports development", including Table S1 and Fig. S4–S6†). In Table 1, the textural properties of the relevant extrudates are summarized.

Pure γ-alumina extrudates were brittle, so binders were needed. Sepiolite alone did not provide enough mechanical strength, and bentonite alone led to hard-to-dry and easy-to-comb extrudates. However, manual extrusions combining boehmite with sepiolite and bentonite had a reasonable drying behavior and acceptable mechanical resistance after calcination, up to a maximum of 70% alumina. Fig. 3 compares the pore size distribution of the pure γ-alumina monolith (black line) with that of the pure clay extrudates (left) and the γ-alumina-rich extrudates (right). As the mesoporosity of the material is mainly related to the voids inside the alumina particles, the pore size of the alumina extrudates with clays was very similar to that of pristine alumina, with a slight decrease at higher clay proportion. In contrast, the specific surface area decreased (see Table 1) due to the smaller volume of mesopores present.

For catalytic screening tests, the selected extrudates were crushed and sieved between 200–500 μm, impregnated with IL-catalyst solution, and tested for the WGS reaction at the same operating conditions for benchmarking against reference γ-alumina particles. The activities of the resulting SILP catalysts are summarized in Fig. 4.

The three carbon-containing support materials, 50C–45S–5K, 50C–50S and 25C–75S, resulted in low conversion levels and were thus discarded for the WGS reaction. This can be

Table 1 Composition and textural properties of the novel shaped ceramic supports

Sample name	Pore volume mL g^{-1}	Surface area m^2 g^{-1}	Porosity %
Al	0.6	196.4	59.9
B	0.1	48.8	21.4
K	0.2	40.1	35.0
S	0.3	66.8	40.2
S-700	0.3	68.4	38.0
S9	1.0	107.9	68.4
S9-PGA	1.7	110.5	78.6
50C–45S–5K	0.6	76.6	45.7
50C–50S	0.5	80.2	44.8
25C–75S	0.5	93.7	45.5
10B–20S–70Al	0.4	180.2	53.8
10B–45S–45Al	0.4	142.8	47.5
20B–40S–40Al	0.3	128.0	44.7
20K–40S–40Al	0.4	127.9	48.8

C = activated carbon, Al = γ-alumina, B = bentonite, K = kaolinite, S = sepiolite. Standard calcination temperature = 550 °C for 4 h.

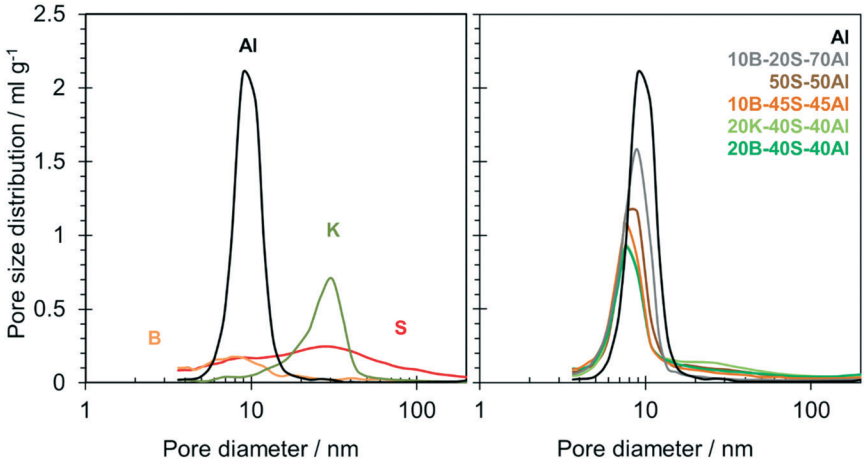

Fig. 3 Pore size distribution of single-component extrudates of γ-alumina and of natural clays (left), and of γ-alumina-rich samples with different proportions of natural clays compared to the pure γ-alumina extrudate (right). Calcination temperature was 550 °C for 4 h.

attributed to the low interaction of the polar IL with the nonpolar carbon leading to the formation of an inhomogeneous IL-catalyst film (poor wettability). This is supported by the fact that the freshly prepared SILP particles from carbonaceous materials did not appear as macroscopically dry and free flowing particles, but rather as sticky particle agglomerations. Also, pure sepiolite samples S9, S9-PGA, S-700 and S resulted in rather poorly active SILP catalysts as compared to the benchmark system. Interestingly, naturally present impurities of sepiolite (see Table S1†) seemed to have a beneficial effect on the performance of S catalyst, prepared with Pansil 100, which was more active than the catalyst prepared using more expensive Pangel S9, having a significantly higher pore volume. Even S9-PGA catalyst, having additional macropores generated by combustion of the activated carbon template, showed lower activity than S catalyst, and they were significantly more fragile. Therefore, Pansil 100 was the selected sepiolite to be used for further investigations, and the generation of extra macropores was initially discarded, despite the beneficial effect found on the activity of S9-PGA catalyst, to avoid excessive fragilization. The calcination at 700 °C improved the crushing strength while keeping the porous structure essentially the same, but led to slightly lower catalytic performance. Overall, the screening revealed that only alumina-containing supports led to high catalytic activities, and in general the activity increased with the content of alumina. The conversion of catalyst 10B–45S–45Al (45 wt% alumina) was doubled when using 10B–20S–70Al (70 wt% alumina, binder content kept as low as possible) from approx. 20 to 40%. Such a value was close to the benchmark of γ-alumina used here and in previous studies.[22,23] This observation also holds for a broader temperature range between 120 and 140 °C (see Fig. S8†). Monoliths with a higher share of alumina were discarded for this application, because they were too brittle and prone to break upon assembly inside the reactor housing or pressurization. Noteworthy, the combination of alumina and binders, keeping most of the γ-alumina properties as support while reducing brittleness, opens the possibility to manufacture the monolithic structures required for application of the monolithic-SILP approach to the WGS reaction and its possible further extension to a membrane reactor concept.

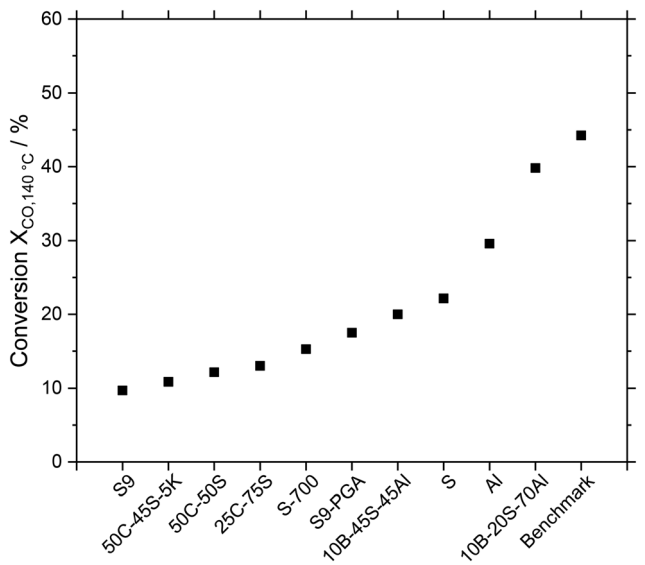

Fig. 4 Average conversion values for CO obtained in Ru-SILP catalyzed WGS for different support materials obtained from extrudates compared to benchmark γ-alumina. T = 140 °C, p = 1 bar, w_{Ru} = 0.02 g $g_{support}^{-1}$, precursor = $[Ru(CO)_3(Cl)_2]_2$, α_{IL} = 0.34, m_{SILP} = 2.0 g, $p_{H_2O}:p_{CO}$ = 2 : 1, F_{total} = 174 mL_N min^{-1}, total run time = 45 h each.

3.3 New mesoporous γ-alumina-rich monolithic support

The promising support composite materials were up-scaled for testing in the monolithic-SILP-WGS process. 10B–20S–70Al monoliths were manufactured by mechanical extrusion with the selected raw materials. The calcination temperature was adjusted between 500 and 850 °C to obtain adequate

chemical, mechanical and textural properties, ensuring the formation of the γ-alumina phase and the dehydration of the silicates structure without formation of low-porosity enstatite phase.[30,31] The calcination at 850 °C significantly improved the mechanical resistance without significant textural and structural changes. Fig. 5 shows the porous distribution (left), the diffraction pattern (right) and a picture of the γ-alumina-rich 10B–20S–70Al monolith.

The majority of the broad diffraction peaks of 10B–20S–70Al calcined at 550 °C were similar to those obtained with pure calcined boehmite and were attributed to the γ-alumina phase. Besides, contributions related to the sepiolite and bentonite clays used as binders were observed. The XRD pattern of the monolith calcined at 850 °C was almost identical regarding the alumina phase. The higher crushing strength of this sample could be attributed to thermal transformations into more resistant phases causing the disappearance of clay diffractions at low 2θ. At the high calcination temperature of 850 °C the porosity was the same (55%) as obtained at the lower calcination temperature, but the size of the mesopores increased slightly from 8.9 to 10.7 nm, resulting in a pore area reduction from 167 to 133 $m^2\ g^{-1}$. The highest calcination temperature was thus selected for the preparation of the monolithic-SILP catalyst due to the larger mesopores as well as its highest mechanical resistance.

A monolithic support from batch 10B–20S–70Al-850 was first dip-coated only with IL for a leaching test. To prevent corrosion problems as found with the IL $[C_4C_1C_1Im]Cl$ (see above), an alternative IL $[C_4C_1Im][EtOSO_3]$ was chosen for this leaching test as a non-corrosive but also hydrophilic IL (which is important for the WGS). The as-prepared monolith was placed in the reactor set-up and exposed to the WGS reaction conditions, including multiple temperature variations (120–160 °C), for a TOS of more than 170 h (data not shown). A weight comparison of the monolith before and after the leaching test (a defined drying procedure was applied both times, which included vacuum extraction of moisture and flushing with inert gas for 24 h) revealed no significant loss in weight (≤0.1 g corresponding to ~0.1 wt% of the total monolith weight). Additionally, analysis of the condensate *via* ICP did not reveal any traces of the sulfur-containing IL. Consequently, leaching of the IL from the monolith could be excluded making the new material promising for the monolith-SILP catalyzed WGS process.

Finally, another monolith from batch 10B–20S–70Al-850 was wet-impregnated with a solution consisting of the Ru-complex dissolved in the standard IL for SILP WGS systems ($[C_4C_1C_1Im]Cl$) in order to obtain the monolithic SILP catalyst for the WGS reaction. The weight gain and resulting Ru loading of the γ-alumina-rich prepared monolith was Δm = 4.62 g, (Ru loading 0.43 g), while it was Δm = 3.24 g (Ru loading 0.30 g) for the SiO_2/SiC monolith (section 3.2). The larger weight gain of the γ-alumina-rich monolith was attributed to the larger total pore volume compared to the SiO_2/SiC monolith. Especially the larger amount of mesopores of the γ-alumina-rich monolith likely immobilized the IL more effectively and prevented leaching due to strong capillary forces in the smaller pores.

3.4 Catalytic test using new monolith supports

The activity results obtained for the Ru-SILP catalyzed WGS process with the 10B–20S–70Al-850 monolithic support at varying temperature and water partial pressure conditions for a total TOS of more than 320 h are summarized in Fig. 6. The top diagram shows the conversion, while the lower diagram depicts the temperature inside the monolith and the water flow rate. Initially, a long phase of decreasing activity was seen, especially throughout the first 150 h. This behavior can be attributed to several phenomena. On the one hand, the reactor and its periphery were maintained under N_2 at the beginning of each experiment (heat-up phase under inert atmosphere). Upon switching to reaction

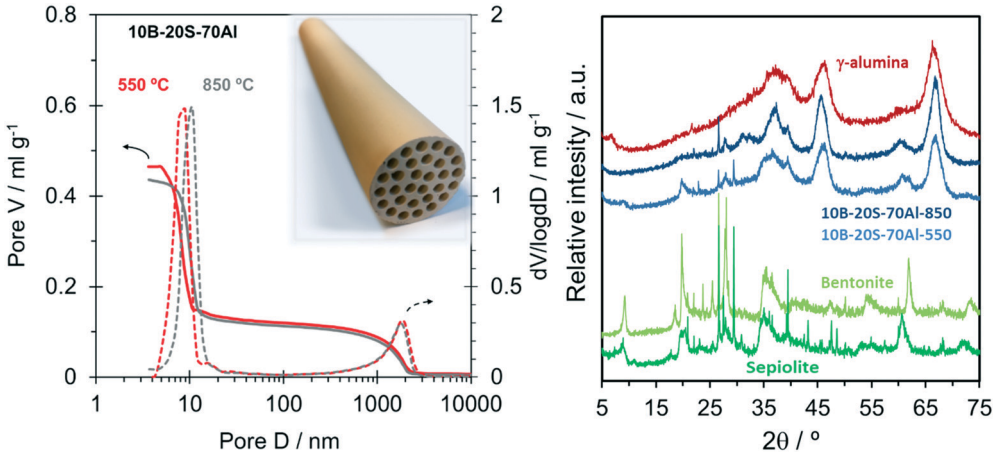

Fig. 5 Pore volume and pore size distribution obtained by MIP for γ-alumina-rich 10B–20S–70Al monolith calcined at 550 and 850 °C (left) with picture of the monolith calcined at 550 °C (inset). XRD patterns of 10B–20S–70Al (blue) and of its individual components calcined at 550 °C: sepiolite (light green), bentonite (dark green), and γ-alumina obtained from boehmite (red).

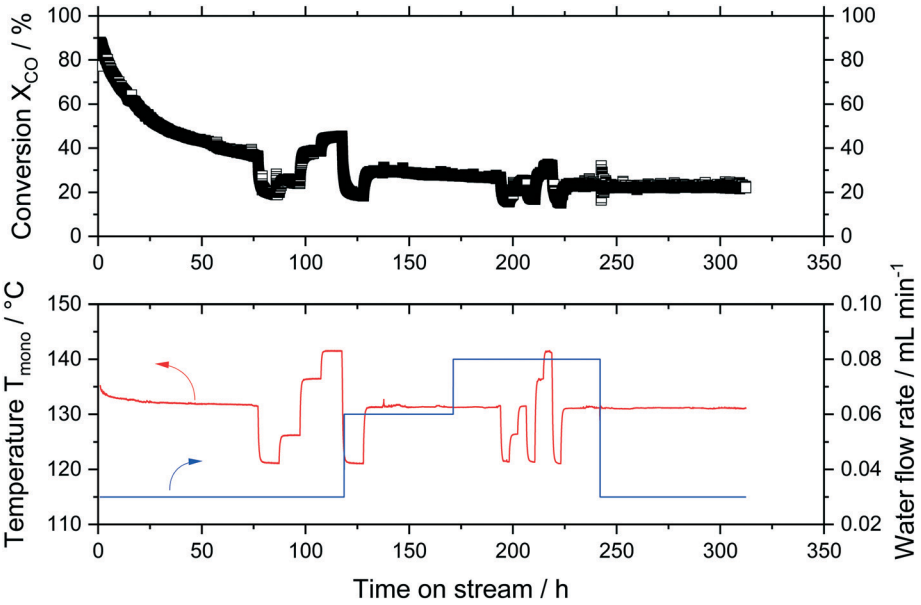

Fig. 6 Ru-SILP catalyzed WGS reaction with the 10B-20S-70Al-850 monolithic support: conversion (black squares, top), temperature inside monolith (red line, bottom) and water flow rate (blue line, bottom). p = 1 bar, precursor = $[Ru(CO)_3(Cl)_2]_2$, $m_{precursor}$ = 1.1 g, IL = $[C_4C_1C_1Im]Cl$, V_{IL} = 3.3 mL, $p_{H_2O}:p_{CO}$ = 2–5 : 1, F_{total} = 174–232 mL_N min^{-1}.

atmosphere, dilution effects result in analytically high conversions. Such behavior, although in smaller dimensions (due to a smaller total reactor volume), could also be seen during the packed-bed experiments with benchmark γ-alumina (see Fig. S7†). On the other hand, an internal restructuring of the active phase due to uptake of water in the IL and subsequent swelling, adsorption of water in the monolithic material and change of wettability may also have played important roles.

After 190 h TOS, steady-state conditions were reached with an average CO conversion of around 30% at 130 °C. The activity of the new monolith was similar to the activity obtained with the analogous SiC monolith, but the former had higher stability, confirming the suitability of the support and encouraging further optimization of the system. Hence, even after 320 h TOS a conversion of 23% was measured at 130 °C with the 10B–20S–70Al-850 monolith. Interestingly, the variation of the water partial pressure did not show any significant effect on the catalytic activity. This strongly supports the hypothesis that the monolith accumulated water during the testing phase, which resulted in constant performance even though the water partial pressure changed significantly, *e.g.* after 245 h TOS, when the partial pressure of water was changed from 0.4 bar to 0.2 bar. Fig. S9† shows pictures of the monolith before and after reaction. After the experiment, the monolith was dried and weighed according to the procedure applied for the IL leaching test, and leaching of the SILP catalysts was discarded. Additionally, the process condensate was used for a qualitative analysis for chloride ions using silver nitrate solution and nitric acid, and chloride was not detected. Only after concentrating the condensate more than a hundred times (from a volume of 1.3 L to 10 mL), traces of chloride ions could be detected. Their quantification by chromatographic analysis indicated a chloride content equivalent to 0.04 mg L^{-1} in the original condensate. Based on this data, leaching of relevant quantities of IL (and catalyst) from the monolith can be excluded despite operating at increased temperatures and water contents.

4 Conclusion & Outlook

Inexpensive ceramic monolithic supports based on γ-alumina and clay binders were designed to carry out the WGS reaction in a structured reactor with immobilized homogeneous Ru-complex catalyst using the SILP concept. By adjusting the chemical composition and pore size distribution, novel γ-alumina-rich monolithic supports were developed with suitable mesoporosity to avoid IL leaching, resistance to withstand the catalyst preparation and operating conditions, and surface chemistry to promote the catalytic activity for the WGS reaction. The designed channeled module was used to perform ultra-low temperature WGS in an easy-to-scale-up system for purification and enrichment of H_2. Moreover, the pore size of the monolith makes it suitable for the application of a polymeric membrane on the external wall for subsequent gas separation.

The study demonstrates the feasibility and potential benefits of a new support for the monolithic-SILP concept and envisages its future use for preparation of an industrially viable membrane-coated monolithic-SILP system applicable for a WGS catalytic membrane reactor.

Conflicts of interest

There are no conflicts of interest to declare.

Acknowledgements

The authors gratefully acknowledge funding by the European Commission within the Horizon 2020-SPIRE project ROMEO (GA 680395). Additional support by the Free State of Bavaria through its funding for the *Energie Campus Nürnberg* (www.encn.de) and by the CSIC Open Access Publication Support Initiative through its Unit of Information Resources for Research (URICI) is acknowledged as well.

References

1 M. Baerns, A. Behr, A. Brehm, J. Gmehling, K.-O. Hinrichsen, H. Hofmann, U. Onken, R. Palkovits and A. Renken, *Technische Chemie*, Wiley-VCH, 2nd edn, 2013, p. 736.
2 N. Schödel, Industrial Hydrogen and Syngas Production - State of the Art and New Development, *Erdöl Erdgas Kohle*, 2016, **132**(2), 70–75.
3 J. R. Jennings, *Catalytic Ammonia Synthesis*, Springer Science +Business Media, LLC, 1991.
4 J. Amphlett, On board hydrogen purification for steam reformation/PEM fuel cell vehicle power plants, *Int. J. Hydrogen Energy*, 1996, **21**(8), 673–678.
5 W. Boll, G. Hochgesand, C. Higman, E. Supp, P. Kalteier, W.-D. Müller, M. Kriebel, H. Schlichting and H. Tanz, Gas Production, 3. Gas Treating, in *Ullmann's Encyclopedia of Industrial Chemistry*, Wiley VCH, 2012.
6 P. C. Ford, The water gas shift reaction: homogeneous catalysis by ruthenium and other metal carbonyls, *Acc. Chem. Res.*, 1981, **14**(2), 31–37.
7 R. Fehrmann, A. Riisager and M. Haumann, *Supported Ionic Liquids: Fundamentals and Applications*, Wiley-VCH, Weinheim, 2014.
8 S. Werner, N. Szesni, R. W. Fischer, M. Haumann and P. Wasserscheid, Homogeneous ruthenium-based water-gas shift catalysts via supported ionic liquid phase (SILP) technology at low temperature and ambient pressure, *Phys. Chem. Chem. Phys.*, 2009, **11**(46), 10817–10819.
9 S. Werner, N. Szesni, M. Kaiser, R. W. Fischer, M. Haumann and P. Wasserscheid, Ultra-Low-Temperature Water-Gas Shift Catalysis using Supported Ionic Liquid Phase (SILP) Materials, *ChemCatChem*, 2010, **2**(11), 1399–1402.
10 H. F. Rase and R. H. James, *Chemical reactor design for process plants*, Wiley, New York, 1977.
11 J. M. Herman, P. J. van den Berg and J. J. F. Scholten, The industrial hydroformylation of olefins with a rhodium-based supported liquid phase catalyst (SLPC), *Chem. Eng. J.*, 1987, **34**(3), 133–142.
12 M. Logemann, P. Wolf, J. Loipersböck, A. Schrade, M. Wessling and M. Haumann, Ultra-low temperature water–gas shift reaction catalyzed by homogeneous Ru-complexes in a membrane reactor – membrane development and proof of concept, *Catal. Sci. Technol.*, 2021, **11**, 1558.
13 V. Palma, D. Pisano and M. Martino, Structured noble metal-based catalysts for the WGS process intensification, *Int. J. Hydrogen Energy*, 2018, **43**(26), 11745–11754.
14 V. Palma, D. Pisano and M. Martino, CFD modeling of the influence of carrier thermal conductivity for structured catalysts in the WGS reaction, *Chem. Eng. Sci.*, 2018, **178**, 1–11.
15 M. T. Kreutzer, F. Kapteijn, J. A. Moulijn and J. J. Heiszwolf, Multiphase monolith reactors: Chemical reaction engineering of segmented flow in microchannels, *Chem. Eng. Sci.*, 2005, **60**(22), 5895–5916.
16 J. A. Moulijn, M. T. Kreutzer, A. T. Nijhuis and F. Kapteijn, Chapter 5 - Monolithic Catalysts and Reactors: High Presicion with Low Energy Consumption, *Adv. Catal.*, 2011, **54**, 249–327.
17 M. Logemann, J. M. Marinkovic, M. Schörner, E. José García-Suárez, C. Hecht, R. Franke, M. Wessling, A. Riisager, R. Fehrmann and M. Haumann, Continuous gas-phase hydroformylation of but-1-ene in a membrane reactor by supported liquid-phase (SLP) catalysis, *Green Chem.*, 2020, **22**(17), 5691–5700.
18 R. Portela, J. M. Marinkovic, M. Logemann, M. Schörner, N. Zahrtman, E. Eray, M. Haumann, E. J. García-Suárez, M. Wessling, P. Ávila, A. Riisager and R. Fehrmann, Monolithic SiC supports with tailored hierarchical porosity for molecularly selective membranes and supported liquid-phase catalysis, *Catal. Today*, DOI: 10.1016/j.cattod.2020.06.045, in press.
19 J. M. Marinkovic, S. Benders, E. J. Garcia-Suarez, A. Weiß, C. Gundlach, M. Haumann, M. Küppers, B. Blümich, R. Fehrmann and A. Riisager, Elucidating the ionic liquid distribution in monolithic SILP hydroformylation catalysts by magnetic resonance imaging, *RSC Adv.*, 2020, **10**(31), 18487–18495.
20 T. Welton, Ionic liquids in catalysis, *Coord. Chem. Rev.*, 2004, **248**(21–24), 2459–2477.
21 J. M. Marinkovic, A. Riisager, R. Franke, P. Wasserscheid and M. Haumann, Fifteen Years of Supported Ionic Liquid Phase-Catalyzed Hydroformylation: Material and Process Developments, *Ind. Eng. Chem. Res.*, 2018, **58**(7), 2409–2420.
22 P. Wolf, M. Aubermann, M. Wolf, T. Bauer, D. Blaumeiser, R. Stepic, C. R. Wick, D. M. Smith, A.-S. Smith, P. Wasserscheid, J. Libuda and M. Haumann, Improving the performance of supported ionic liquid phase (SILP) catalysts for the ultra-low-temperature water–gas shift reaction using metal salt additives, *Green Chem.*, 2019, **21**(18), 5008–5018.
23 P. Wolf, M. Logemann, M. Schörner, L. Keller, M. Haumann and M. Wessling, Multi-walled carbon nanotube-based composite materials as catalyst support for water–gas shift and hydroformylation reactions, *RSC Adv.*, 2019, **9**(47), 27732–27742.
24 S. Werner, Ultra-Low Temperature Water-Gas Shift Reaction with Supported Ionic Liquid Phase (SILP) Catalysts, *Dissertation*, Friedrich-Alexander-Universität Erlangen-Nürnberg, 2011.

25 J. Bortolozzi, R. Portela, P. Ávila, V. Milt and E. Miró, Novel Ni-Ce-Zr/Al_2O_3 Cellular Structure for the Oxidative Dehydrogenation of Ethane, *Catalysts*, 2017, **7**(11), 331.
26 T. Bauer, R. Stepic, P. Wolf, F. Kollhoff, W. Karawacka, C. R. Wick, M. Haumann, P. Wasserscheid, D. M. Smith, A.-S. Smith and J. Libuda, Dynamic equilibria in supported ionic liquid phase (SILP) catalysis: in situ IR spectroscopy identifies [Ru(CO)xCly]n species in water gas shift catalysis, *Catal. Sci. Technol.*, 2018, **8**(1), 344–357.
27 KYOCERA Corporation, *Technical Data - Thermal Conductivity*, 2010, https://global.kyocera.com/prdct/fc/list/tokusei/denndou/index.html (visited 31.10.2019).
28 Iron Boar Labs Ltd., *Material Properties Database*, 2009, https://www.makeitfrom.com/material-properties/Alumina-Aluminum-Oxide-Al2O3 (visited 31.10.2019).
29 F.-Y. Ma, in *Pitting Corrosion*, ed. N. Bensalah, IntechOpen, 2012.
30 H. Nagata, On Dehydration of Bound Water of Sepiolite, *Clays Clay Miner.*, 1974, **22**(3), 285–293.
31 R. Portela, I. Jansson, S. Suárez, M. Villarroel, B. Sánchez and P. Avila, Natural silicate-TiO 2 hybrids for photocatalytic oxidation of formaldehyde in gas phase, *Chem. Eng. J.*, 2017, **310**, 560–570.